

Anisotropic properties of acoustically induced electric polarization in soft biological fibrous tissues

Junna Kikuchi^{1†‡}, Yuki Sakakura¹, and Kenji Ikushima^{1*} (¹Tokyo Univ. A & T)

1. Introduction

Soft biological fibrous tissues, such as tendon, muscle, and blood vessel wall, are composed of fibrous proteins, such as collagen, elastin, and myosin. The degree of fiber orientation is an important indicator for evaluating the quality of fibrous tissues because it contributes to the toughness of the tissues. Because the standard ultrasound echo method is usually limited to the evaluation of mechanical and geometric properties,^{1,2)} the development of new measurement schemes is eagerly awaited in clinical setting.

Recently, we have proposed a unique ultrasonic method to measure the acoustically induced electric polarization.³⁾ The principle of this method is based on the generation and detection of acoustically stimulated electromagnetic (ASEM) response through electro- or magneto-mechanical coupling of materials. We have demonstrated that distinct electric polarization is generated by ultrasound waves in soft biological fibrous tissues, such as Achilles tendon, aortic wall, and aortic valve, whereas polarization is small in non-fibrous tissues, such as adipose tissue and myocardium.⁴⁾ The ASEM signal responds linearly to the applied acoustic pressure, indicating that fibrous tissues exhibit piezoelectric polarization.

The piezoelectricity in biological tissues was first discovered in dehydrated femoral cortex.⁵⁾ The origin of this piezoelectricity is thought to be highly oriented collagen fibers. After this discovery, the piezoelectricity in dehydrated soft fibrous biological tissues such as Achilles tendon, aortic wall, trachea, and intestine was reported.^{6,7)} Anisotropic properties of piezoelectric polarization are determined by the crystal symmetry. Approximating the fiber structure to uniaxial symmetry with the direction of fiber orientation (the 3-axis) as the principal axis, piezoelectricity is inferred to follow the piezoelectric tensor with the C_6 symmetry:

$$\begin{matrix} 0 & 0 & 0 & d_{14} & d_{15} & 0 \\ 0 & 0 & 0 & d_{15} & -d_{14} & 0 \\ d_{31} & d_{31} & d_{33} & 0 & 0 & 0 \end{matrix}$$

In fact, the stress-induced polarization of dehydrated Achilles tendon is suggested to be anisotropic, following the piezoelectric tensor of C_6 symmetry. The shear term d_{14} is more than one order of magnitude larger than the other components.⁶⁾ However, the consequence is only indicated by the results of tensile and compression testing in well-

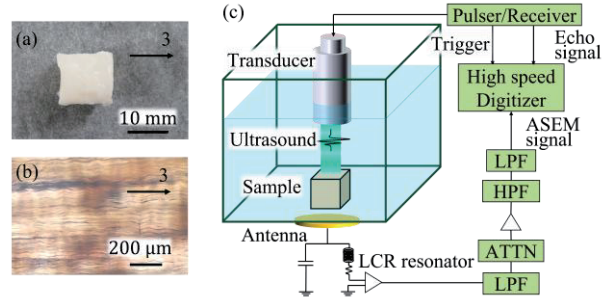


Fig. 1 (a) Photograph of the Achilles tendon sample. (b) Microphotograph of the Achilles tendon. (c) Schematic illustration of the ASEM measurement setup.

dehydrated biological samples. The advantage of the ASEM method is that the acoustically induced polarization originated from piezoelectricity is measured even in wet tissues owing to high-frequency ultrasound modulation. In this paper, we use the ASEM method to investigate the anisotropic feature of the polarization for the non-shear terms of piezoelectric tensor in fibrous tissues under wet conditions and confirm its consistency with the piezoelectric tensor of C_6 symmetry.

2. Experimental Setup

A bovine Achilles tendon was cut into a cube 10 mm on each side (Fig. 1(a)). The direction of its fiber orientation was confirmed from a slice extracted around the sample and was defined as 3-axis (Fig. 1(b)). The schematic illustration of measurement setup is shown in Fig. 1(c). The sample set in plastic holder was submerged in deionized water in a water tank. A planer transducer (peak frequency: 3-4 MHz) and the sample holder were attached to an XYZ stage. ASEM signal was detected by a capacitive metal (Cu) plate antenna coupled with an LCR resonator. The center frequency of the LCR resonator was tuned to ultrasound frequency to detect induced polarization alternating with ultrasound frequency. This antenna was placed at the bottom or the side of the water tank. The detected ASEM signal was amplified by 92 dB and averaged over 3.0×10^4 pulses. The ASEM signal amplitude is proportional to the induced charge on the surface of the antenna.⁴⁾

Figure 2 shows the schematic of the measurement setups for d_{33} and d_{13} components (d_{33} and d_{13} setups). Ultrasound was irradiated to the direction of fiber orientation (3-axis). The antenna was placed at the bottom and the side of the

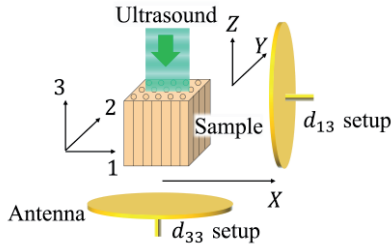


Fig. 2 Schematic of the measurement setup for d_{33} and d_{13} terms. The illustration of the water tank is omitted for clarity. The 123 and XYZ coordinate systems define the crystal axes of tendon and spatial coordinates, respectively.

water tank in the d_{33} and the d_{13} setups, respectively.

Suppose that the induced polarization is parallel to the normal vector of the metal plate antenna. The induced charge on the antenna should be maximized when the sample is positioned over the center of the antenna. The induced charge decreases as the sample moves away from the center of the antenna. Therefore, the signal amplitude is expected to exhibit a convex upward curve as a function of off-center position. In contrast, for the polarization perpendicular to the normal vector of the antenna, the induced charge on the antenna should be minimized when the sample is positioned over the center of the antenna. Therefore, the signal amplitude is expected to exhibit a convex downward curve as a function of off-center position. The one-dimensional (1D) profile in relation to the antenna and the sample position allows us to identify the direction of polarization.

3. Results and discussion

The 1D profile of the ASEM signal amplitude along the X -axis in the d_{33} setup is shown in **Fig. 3(a)**, where ΔX is off-center position. The convex upward curve indicates that polarization occurs in the 3-axis direction (the direction of fiber orientation). To provide further assurance, we also measured the 1D profile along the Z -axis in the d_{13} setup, where ΔZ is off-center position in the Z -axis. The obtained convex downward curve (Fig. 3(b)) strongly supports that the polarization vector is oriented in the 3-axis direction.

The other piezoelectric components are also investigated by measuring the 1D profile of ASEM signal amplitude along the Y -axis, where ΔY is off-center position in the Y -axis. In the 1D profile in the d_{13} setup, we observe a convex upward curve (Fig. 3(c)), whereas no clear convex curve is observed in the d_{31} setup (Figs. 3(d)).

Because the ASEM signal amplitude is proportional to the magnitude of piezoelectric

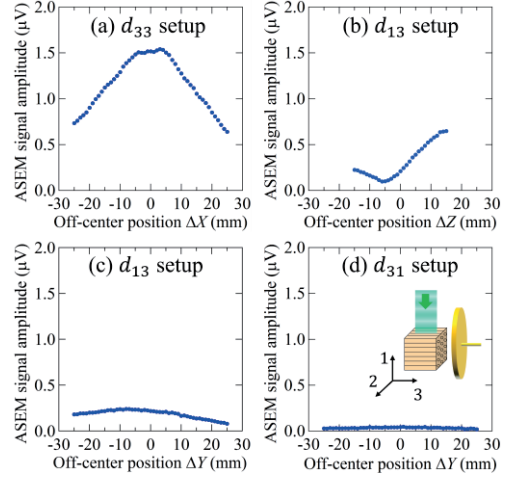


Fig. 3 ASEM signal amplitude as a function of off-center position, (a) ΔX in the d_{33} setup, (b) ΔZ in the d_{13} setup, (c) ΔY in the d_{13} setups, and (d) ΔY in the d_{31} setup. The inset in (d) represents the schematic of the d_{31} setup.

components,^{3,4)} simply considered, d_{33} is the largest among the non-shear terms. Though not shown here, similar results are also obtained in skeletal muscle. In Ref. 6, piezoelectric measurements of dehydrated tendon tissues by tensile and compression testing indicate that d_{33} is similar in magnitude to d_{31} , and results for the zero-component in C_6 symmetry have not been reported. In our evaluation of piezoelectricity by the ASEM method, we should pay attention to the possibility that a uniform acoustic pressure is not necessarily applied to the entire sample. This may result in unintended shear stress, possibly contributed by polarization generation through the large d_{14} component.

4. Conclusion

We investigated the anisotropic properties of acoustically induced electric polarization in soft biological fibrous tissues. In the non-shear terms, the polarization tends to occur in the direction of fiber orientation.

References

- 1) O. C. Dams, I. H. F. Reininga, J. L. Gielen, I. van den Akker-Scheek, and J. Zwerver, *Injury* **48**, 2383 (2017).
- 2) P. Peetrons, *Eur. Radiol.* **12**, 35 (2002).
- 3) K. Ikushima, *Jpn. J. Appl. Phys.* **62**, SJ0802 (2023).
- 4) K. Ikushima, T. Kumamoto, K. Ito, and Y. Anzai, *Phys. Rev. Lett.* **123**, 238101 (2019).
- 5) E. Fukada and I. Yasuda, *J. Phys. Soc. Jpn.* **12**, 1158 (1957).
- 6) E. Fukada and I. Yasuda, *Jpn. J. Appl. Phys.* **3**, 117 (1964).
- 7) E. Fukada and K. Hara, *J. Phys. Soc. Jpn.* **26**, 777 (1969).